Journal of Food Engineering 300 (2021) 110513

Contents lists available at ScienceDirect

Journal of Food Engineering

journal homepage: http://www.elsevier.com/locate/jfoodeng

Influence of food additives on blister formation in tinplate can of coconut milk

Duangkamol Promlok [a,b], Noparat Kanjanaprayut [c], Nuntawat Kiatisereekul [c], Ratana Chanthateyanonth [d], Manthana Jariyaboon [b,e,*]

[a] Polymer Science and Technology Program, Faculty of Science, Mahidol University, Phuttamonthon, Nakhon Pathom, 73170, Thailand
[b] Center for Surface Science and Engineering, Faculty of Science, Mahidol University, Phuttamonthon, Nakhon Pathom, 73170, Thailand
[c] Corrosion Technology Department, Thai-French Innovation Institute, King Mongkut's University of Technology North Bangkok, Bangsue, Bangkok, 10800, Thailand
[d] Rubber Technology Research Centre, Faculty of Science, Mahidol University, Phuttamonthon, Nakhon Pathom, 73170, Thailand
[e] Department of Chemistry, Faculty of Science, Mahidol University, Ratchathewi, Bangkok, 10400, Thailand

ARTICLE INFO

Keywords:
Blister
Coconut milk
Tinplate can
Food additive

ABSTRACT

Blistering is one of the major issues in processed canned coconut milk that contain several food additives. The goal of this work is to investigate the effect of five different food additives, guar gum, sodium carboxymethyl cellulose (CMC), polysorbate 60 (tween 60), citric acid ($C_6H_8O_7$), and sodium metabisulfite ($Na_2S_2O_5$), on blister formation in epoxy-phenolic coated tinplate cans using electrochemical impedance spectroscopy (EIS) and surface microscopy. Cathodic stripping at −6 V (Ag/AgCl) for 30 min was applied in order to provoke blisters. The results revealed that the sterilizing process deteriorated the coating performance, however, without food additives, blisters did not form even after an applied potential. $Na_2S_2O_5$ and CMC were the most aggressive food additives for which blisters were observed for both non-sterilized and sterilized conditions. Na^+ ions, together with water and oxygen in the solution, permeated through the coating initiating and accelerating the blister formation.

1. Introduction

Thailand is one of top ten nations in the world producing coconut. Coconut milk is one of the major coconut products since it is the main ingredient in many traditional Asian cuisines. However, fresh coconut milk is easily spoiled within a few hours at room temperature due to a high fat content. To extend stability and shelf life, the coconut milk can be preserved and packaged in the form of processed coconut milk. This is achieved by adding food additives and packaging under sterilizing conditions (Marikkar and Madurapperuma, 2012). Several types of food additives are added in the processed coconut milk: stabilizer (e.g. guar gum, sodium carboxymethyl cellulose (CMC)), emulsifier (e.g. polysorbate 60 (tween 60)), antioxidant (e.g. citric acid ($C_6H_8O_7$)), preservative and anti-browning agents (e.g. sodium metabisulfite ($Na_2S_2O_5$)).

The processed coconut milk is commonly packed in a tinplate can (tin coated steel) due to the non-toxicity of tin salts, low weight, and high mechanical strength, as well as easy recycling (Page et al., 2003). Furthermore, this method of packaging also prolongs the shelf-life (>2 years) compared to other types such as plastic bag or paper-laminated box (Jafari et al., 2018). However, the drawbacks of metallic cans are cosmetic, blistering/corrosion problems on both the inside and outside of the can. If the problem occurs inside the can, it will of course directly deteriorate the quality of the food products (Charbonneau, 1997, 2001; Jafari et al., 2018; Kontominas et al., 2006). The tinplate can is usually coated with lacquer (organic coating) in order to avoid the contact between food and metal, as well as to minimize corrosion issues.

Over the past decade, failures of food/beverage cans have been investigated. Combinations of several techniques have been used to identify the problems such as surface microscopy (e.g. SEM/EDS)/spectroscopy (e.g. XPS), and electrochemical method (e.g. EIS) (Charbonneau, 1997, 2001; Dey and Agrawal, 2018; Doherty and Sykes, 2004; Freire et al., 2016; Kogure et al., 2019; Kontominas et al., 2006; Maharatanaviroj et al., 2016; Pournaras et al., 2008; Veríssimo et al., 2016; Xia et al., 2012; Zhou et al., 2013). Different types of failures have been found: (i) black discoloration of metal sulfides, oxides, or phosphates on the can or on the food product due to the reaction between exposed iron or tin from the can with the food constituents; (ii) stress corrosion cracking (SCC) involving corrosion at stressed areas in the

* Corresponding author. Department of Chemistry, Faculty of Science, Mahidol University, Ratchathewi, Bangkok, 10400, Thailand.
E-mail address: manthana.jar@mahidol.ac.th (M. Jariyaboon).

https://doi.org/10.1016/j.jfoodeng.2021.110513
Received 18 August 2020; Received in revised form 22 January 2021; Accepted 25 January 2021
Available online 2 February 2021

Fig. 1. A three-piece tinplate can.

container (e.g. side seam weld of welded can, body beads, and bottoms of two-piece can); (iii) pitting corrosion due to a high dissolution rate of iron at the defects; (iv) filiform corrosion as a result of microcracks in the coating at high relative humidity; and (v) enamel adhesion failure which leads to blister formation.

Several works (Charbonneau, 2001; Dey and Agrawal, 2018; Freire et al., 2016; Grassino et al., 2010; Kontominas et al., 2006; Maharatanaviroj et al., 2016; Xia et al., 2012; Zhou et al., 2013) have been dedicated on failures of the lacquered tinplate cans. Epoxy-phenolic lacquer has been commonly applied on the internal surface of the tinplate can. Internal blister and corrosion have been found and their extent depended on defects or porosity of lacquer, coating weight of lacquer, pH and type of the food product, contaminant on the surface, temperature and duration of storage, as well as temperature during sterilizing process.

In Thailand, the blistering and corrosion problems still exist in the lacquered tinplate cans packed with processed coconut milk containing food additives. The cause of the problems remains unclear. Thus, our goal is to investigate effect of food additives on blister formation of the lacquered tinplate cans using electrochemical impedance spectroscopy (EIS) and scanning electron microscopy (SEM). In order to reflect the real usage, sterilizing conditions, concentrations and types of food additives, and type of can were supplied by the Thai processed coconut milk can industry in the present work. A three-piece epoxy-phenolic coated tinplate can was investigated with five different food additives: guar gum, sodium carboxymethyl cellulose (CMC), polysorbate 60 (tween 60), citric acid ($C_6H_8O_7$), and sodium metabisulfite ($Na_2S_2O_5$).

2. Materials and method

2.1. Tinplate can

The commercial lacquered-tinplate can was provided by Lohakij Rung Charoen Sub Co., Ltd., Thailand. It was a three-piece beaded can with an easy open top, as displayed in Fig. 1. A diameter and a height of the can were 76.2 mm and 112.7 mm, respectively. Tinplate sheet with differential tin coating masses, type D1.10/2.80 gm^{-2}, was used to produce a body of the can. The base and top of the can were made of tin free plate. One layer of epoxy-phenolic lacquer was applied on the internal surface of the tinplate can with a film weight and thickness of 11.5–13.0 gm^{-2} and 10 μm, respectively.

Table 1
Concentrations and pHs of five food additives.

Food additives	Concentration (wt.%)	pH
Guar gum	0.60	6.1
CMC	0.40	7.2
Tween 60	0.20	4.5
Citric acid	0.03	3.2
$Na_2S_2O_5$	0.02	4.9

2.2. Food additives

The five different food additives used in this work were guar gum, CMC, tween 60, citric acid, and $Na_2S_2O_5$. Guar gum, CMC, and $Na_2S_2O_5$ were purchased from Chemipan Corporation Co., Ltd. Tween 60 and citric acid were purchased from Sigma-Aldrich and RCI Labscan Co., Ltd., respectively. A solution of each food additive was prepared using distilled water as a solvent. Concentration of each food additive solution and its pH are illustrated in Table 1. Types of food additives and their concentrations were recommended by the Thai processed coconut milk can industry, Lohakij Rung Charoen Sub Co., Ltd. The concentration of each food additive studied in this work is the highest concentration used in the real processed coconut milk can industry. pHs of food additive solutions were measured using a pH meter (MI150, Milwaukee).

2.3. Sample preparation and sterilizing conditions

The lacquered-tinplate cans were separately packed with 410 g of each food additive at concentration shown in Table 1. The filling temperature of the single solution was 28 °C ± 2 °C. After that, the top end of the can was double seemed. The cans were retorted at 121.1 °C for 90 min. After that, the cans were cooled down by reducing the temperature to 30 °C with a cooling rate of 0.75 °C/min. This process was based on the sterilizing process used by the Thai processed coconut milk can industry, Lohakij Rung Charoen Sub Co., Ltd. After the cool down process, the cans were left at room temperature for 24 h before EIS measurements.

2.4. EIS measurement

All EIS measurements were carried out using a PGSTAT302N potentiostat (Metrohm, Autolab). A common three-electrode cell was used; A whole lacquered-tinplate can packed with each food additive was used as a working electrode; Ag/AgCl and Pt rod were used as reference and counter electrodes, respectively. The height of food additive solution in the lacquered-tinplate can was 98 mm. The EIS measurements were performed at the open circuit potential with ±10 mV amplitude over a range of frequency of 0.01 Hz–100 kHz.

In order to obtain a better understanding of how each food additive promptly affected blister formation, a coating delamination was accelerated using a cathodic disbondment method; A cathodic potential (cathodic stripping) of −6 V (Ag/AgCl) was applied to the lacquered-tinplate cans containing each food additive solution for 30 min (optimized time). After that, the cans were left at room temperature for 24 h and the EIS measurements were then carried out as described above. The applied voltage of −6 V (Ag/AgCl) was the voltage used to creating cathodic delamination or blister formation of epoxy-phenolic coating (Maharatanaviroj et al., 2016; Upadhyay et al., 2020) and it is also the applied voltage used for evaluating the coating performance in the Thai processed coconut milk can industry.

All EIS measurements were performed in a naturally-aerated

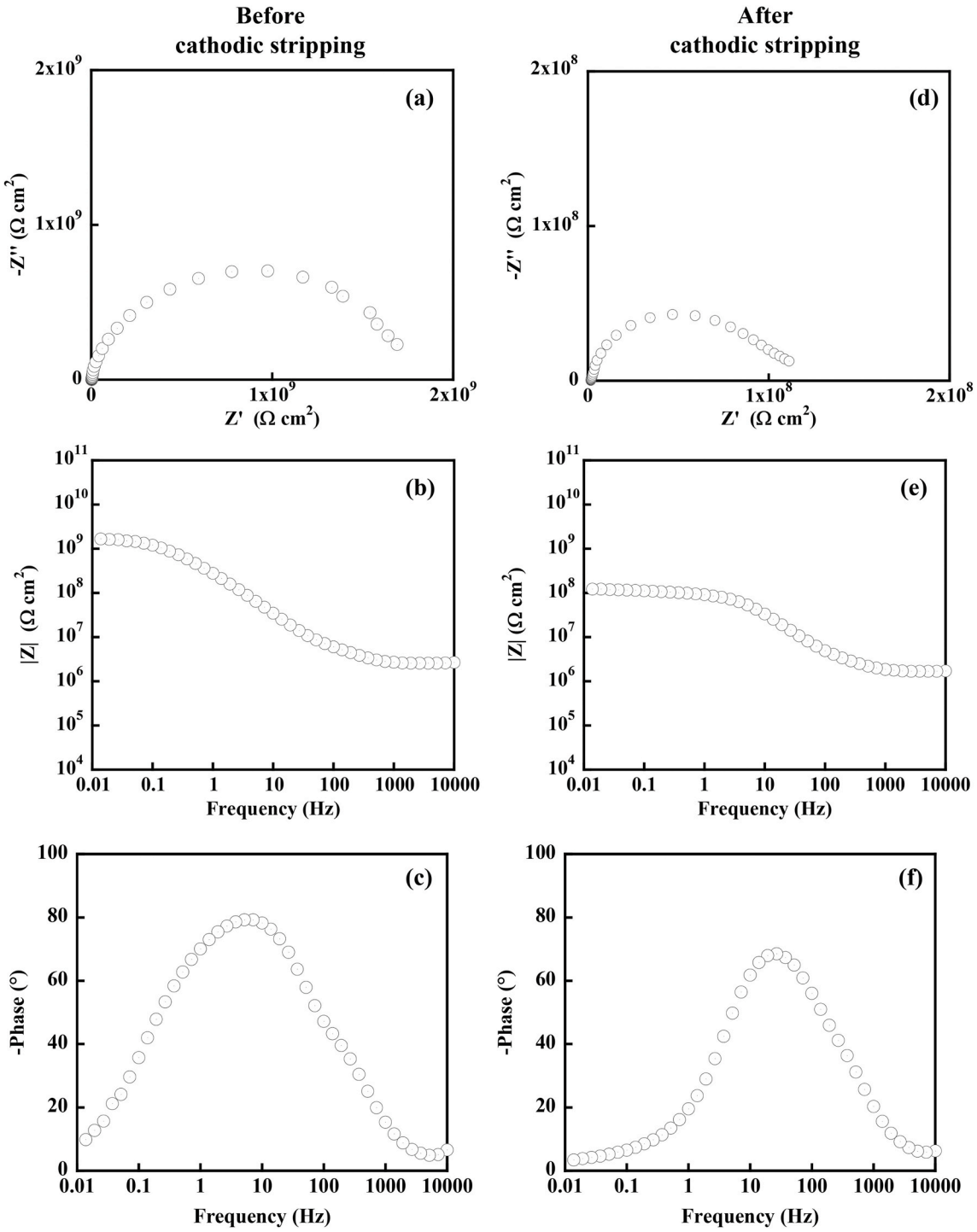

Fig. 2. Impedance diagrams of distilled water in epoxy-phenolic coated tinplate can for non-sterilized condition. (a) Nyquist, (b) Bode modulus, (c) Bode phase plots before cathodic stripping, (d) Nyquist, (e) Bode modulus, and (f) Bode phase plots after cathodic stripping at −6 V (Ag/AgCl).

condition at room temperature in triplicate for both sterilized and non-sterilized conditions. Impedance diagrams were plotted as Nyquist and Bode plots and equivalent circuits were determined.

2.5. Surface morphology analysis

Macroscopic images of internal surfaces of the lacquered-tinplate cans were taken using a digital camara (Fuji X10). Cross-sectional surfaces were examined, at accelerating voltage of 20 kV, using a field emission scanning electron microscope (FE-SEM, Nova Nanosem 450/FEI) equipped with energy dispersive X-ray spectroscopy (EDS, Bruker XFlash 6130). Chemical compositions were determined using EDS at accelerating voltage of 20 kV. The samples for the SEM analysis were coated with gold.

2.6. Statistical method for data processing

In order to check the influence of individual parameters employed in the electrochemical test on the degradation of epoxy-phenolic lacquer, the analysis of variance (ANOVA, $p < 0.05$) was performed. Comparison

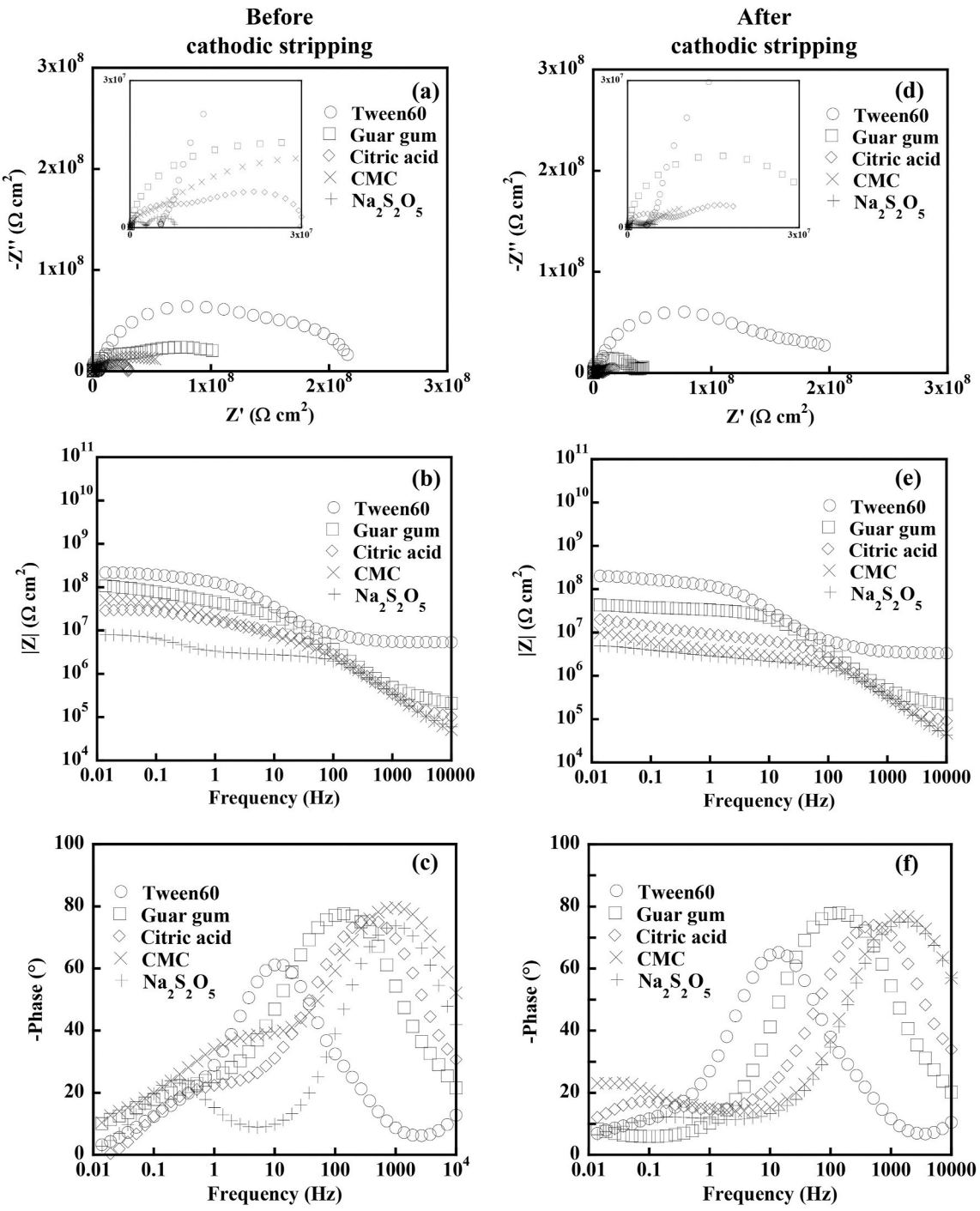

Fig. 3. Impedance diagrams of five food additives in epoxy-phenolic coated tinplate cans for non-sterilized condition. (a) Nyquist, (b) Bode modulus, (c) Bode phase plots before cathodic stripping, (d) Nyquist, (e) Bode modulus, and (f) Bode phase plots after cathodic stripping at −6 V (Ag/AgCl).

among groups was made by one-way ANOVA with Turkey's test.

3. Results

3.1. Non-sterilized condition

The epoxy-phenolic coated tinplate cans were separately filled with distilled water, which was used as a control electrolyte, and with each food additive at concentration shown in Table 1. The cans were kept at room temperature for 24 h. EIS measurements were then carried out both before and after cathodic stripping at −6 V (Ag/AgCl).

3.1.1. Control electrolyte

The impedance diagrams of the epoxy-phenolic coated tinplate can containing distilled water are illustrated in Fig. 2. Nyquist plots of both before and after cathodic stripping showed a semicircle of one time constant, as displayed in Fig. 2a and d, respectively. This represented the intact coating characteristics (Amirudin and Thieny, 1995; Grundmeier et al., 2000; Popov et al., 1993; Wang et al., 2014; Xia et al., 2012; Zhou et al., 2013). However, a reduction of the diameter of the Nyquist plot was observed after cathodic stripping. The pure capacitive behavior of the coating in the distilled water could not be observed, indicating that the coating was wetted by the electrolyte. Furthermore, it was due to the fact that the measurements were carried out on the whole beaded cans.

Bode modulus plots of before and after cathodic stripping are illustrated in Fig. 2b and e, respectively. The high frequency region explains the local surface defects formed on the coating by corrosion, the mid frequency region represents the reaction involved within the film, and the low frequency region reveals the behavior occurring because of corrosion in the metal/film interface (Rikhari et al., 2016). Bode plot of an intact coating displayed as a straight line with a negative slope indicates the complete block between metal substrate and electrolyte (Feng and Frankel, 2016; Zhang et al., 2018). In this work, Bode plot was not the straight line. It suggested that water penetrated the coating through pores. After cathodic stripping, |Z| values at 0.01 Hz decreased from 10^9 Ω cm^2 to 10^8 Ω cm^2. However, high impedance value (>10^7 Ω cm^2) was observed, indicating that the epoxy-phenolic coating was intact and showed a protective performance after being exposed to distilled water, and even after cathodic stripping. Upadhyay et al. (2020) showed that blister formation or delamination of epoxy coating occurred at $|Z| < 10^7$ Ω cm^2.

Bode phase plots before and after cathodic stripping are illustrated in Fig. 2c and f, respectively. Before cathodic stripping, a broad bell-shaped curve with a maximum phase angle close to 80° was observed, whereas after cathodic stripping, a narrower bell-shaped curve with a slight shift of maximum peak to higher frequency and a lower maximum angle was seen, indicating that the epoxy-phenolic layer was soaked with water after the applied potential. As the solution gradually permeated into the coating, the phase angle at a given frequency decreased due to the parallel capacitance characteristic of the coating (Li et al., 2014; Zhang et al., 2018).

3.1.2. Effect of food additives

Guar gum, CMC, tween 60, citric acid, and $Na_2S_2O_5$ were separately filled in the epoxy-phenolic coated tinplate cans with the concentrations shown in Table 1. The impedance diagram of each food additive is illustrated in Fig. 3. Generally, for both before and after cathodic stripping, the Nyquist plots showed two-semicircle feature of two time constants, as seen in Fig. 3a and d, respectively. The diagram at high frequency represented the coating behavior and that at low frequency represented the behavior of the coating/metal interface. Thus, it suggested that all food additives penetrated through the epoxy-phenolic coating and approached the coating/metal interface. Tween 60 showed the largest diameter of Nyquist plot, at both the high and low frequency range, compared with other additives. In addition, tween 60 was the only food additive showing a larger arc chord at high frequency of coating than that of the arc chord at low frequency of the coating/metal interface. Thus, the epoxy-phenolic coating still had a high resistivity to electrolyte penetration after contacting with tween 60, with only a little tween 60 penetrating into the coating and reaching the coating/metal interface. After cathodic stripping, the diameter of the Nyquist plot of tween 60 remained almost the same, while the diameters of the capacitive loops of guar gum, CMC, citric acid, and $Na_2S_2O_5$ significantly reduced, suggesting more electrolyte penetration.

Bode modulus plots of all additives for both before and after cathodic stripping are displayed in Fig. 3b and e, respectively. After cathodic stripping, a reduction of |Z| values at 0.01 Hz of all additives, except tween 60, was clearly seen. Tween 60 showed the highest value followed by guar gum, citric acid, CMC, and $Na_2S_2O_5$.

For the Bode phase plots of before and after cathodic stripping, as illustrated in Fig. 3c and f, respectively, two bell-shaped peaks were observed for all additives except tween 60. The diagram of tween 60 was similar to that of distilled water, suggesting that the electrochemical process at the coating/metal interface was insignificant. Breakpoint frequency (f_b), the frequency at 45-phase angle, of $Na_2S_2O_5$ and CMC shifted to a higher frequency compared with citric acid, guar gum, and tween 60, indicating that ions from $Na_2S_2O_5$ and CMC could penetrate into the coating more than citric acid, guar gum, and tween 60. The breakpoint frequency pointed to an increase in the electrochemically-active surface area (Jianguo et al., 2005).

Table 2
Blister formation in epoxy-phenolic coated tinplate cans with non-sterilized condition.

Food additives	Blisters (non-sterilized condition)	
	Before cathodic stripping	After cathodic stripping
Distilled water (control)	No	No
Tween 60	No	No
Guar gum	No	No
Citric acid	No	No
CMC	No	Yes (large)
$Na_2S_2O_5$	No	Yes (small)

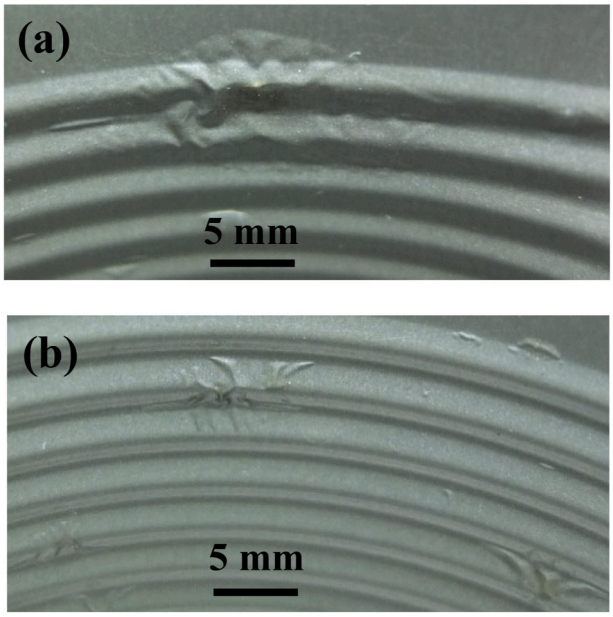

Fig. 4. Macroscopic images of blisters in non-sterilized cans containing (a) CMC and (b) $Na_2S_2O_5$ after cathodic stripping at −6 V (Ag/AgCl).

3.1.3. Surface morphology analysis

Table 2 illustrates a summary of blister formation investigated by visual observation for non-sterilized cans containing distilled water and five different food additives and for both before and after cathodic stripping at −6 V (Ag/AgCl). Blisters were seen in the cans containing CMC and $Na_2S_2O_5$, after cathodic stripping. Macroscopic images of blisters are displayed in Fig. 4. CMC showed larger blisters with a lower concentration, whereas $Na_2S_2O_5$ showed smaller blisters with a higher concentration.

3.2. Sterilized conditions

In the case of sterilized conditions, the epoxy-phenolic coated tinplate cans were separately packed with distilled water and with each food additive at concentration shown in Table 1. They were retorted at 121 °C for 90 min, as described in Section 2.3. EIS measurements were then carried out for both before and after cathodic stripping at −6 V (Ag/AgCl).

3.2.1. Control electrolyte

The impedance diagram of the epoxy-phenolic coated tinplate can containing distilled water after sterilization process is illustrated in Fig. 5. Generally, it was similar to that of the non-sterilized condition, both before and after cathodic stripping. Nevertheless, the diameter of the semicircle of the Nyquist plot and |Z| values at 0.01 Hz decreased with a narrower peak of the Bode phase plot. This suggested that the efficiency of coating was degraded by the sterilization process, even

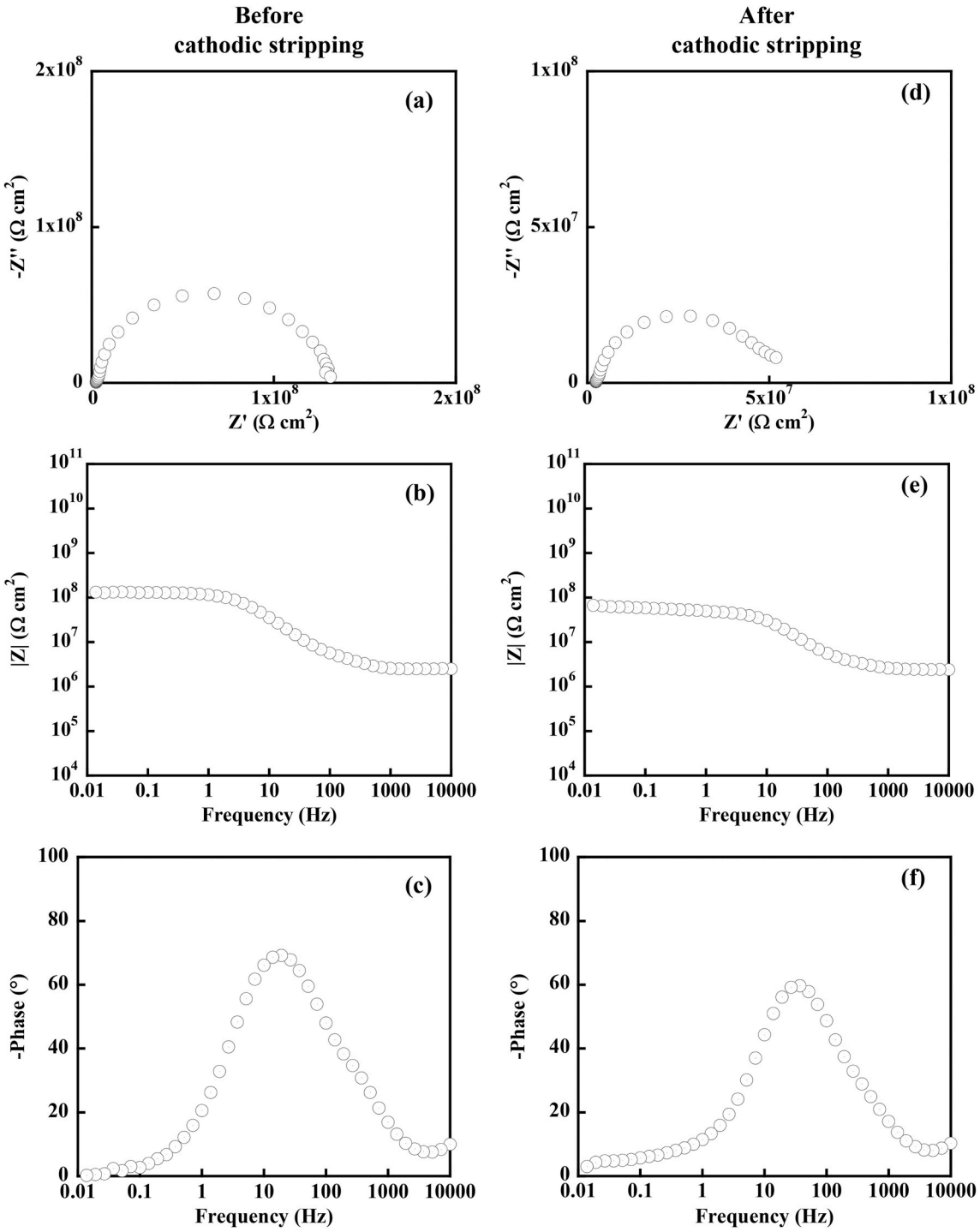

Fig. 5. Impedance diagrams of distilled water in epoxy-phenolic coated tinplate cans for sterilized conditions. (a) Nyquist, (b) Bode modulus, (c) Bode phase plots before cathodic stripping, (d) Nyquist, (e) Bode modulus, and (f) Bode phase plots after cathodic stripping at −6 V (Ag/AgCl).

using distilled water.

3.2.2. *Effect of food additives*

Fig. 6 illustrates the impedance diagram of the epoxy-phenolic coated tinplate can containing different food additives in the case of sterilized conditions. In general, the results were similar to the non-sterilized condition, with a reduction of the coating performance.

Two capacitive loops were also observed with a decrease in their diameters compared with non-sterilized condition, especially for CMC and $Na_2S_2O_5$ after cathodic stripping, as illustrated in Fig. 6a and d. Fig. 6b and e shows that CMC and $Na_2S_2O_5$ gave the lowest |Z| values at 0.01 Hz of approximately 10^6 Ω cm^2. According to the Bode phase plots, as shown in Fig. 6c and f, peaks at high frequency of CMC and $Na_2S_2O_5$ shifted to a higher frequency than those of others, especially after cathodic stripping.

3.2.3. *Surface morphology analysis*

A summary of blister formation observed by visual inspection in the case of sterilized conditions is shown in Table 3. The results were similar to that of non-sterilized condition; Blisters were noticed in the cans

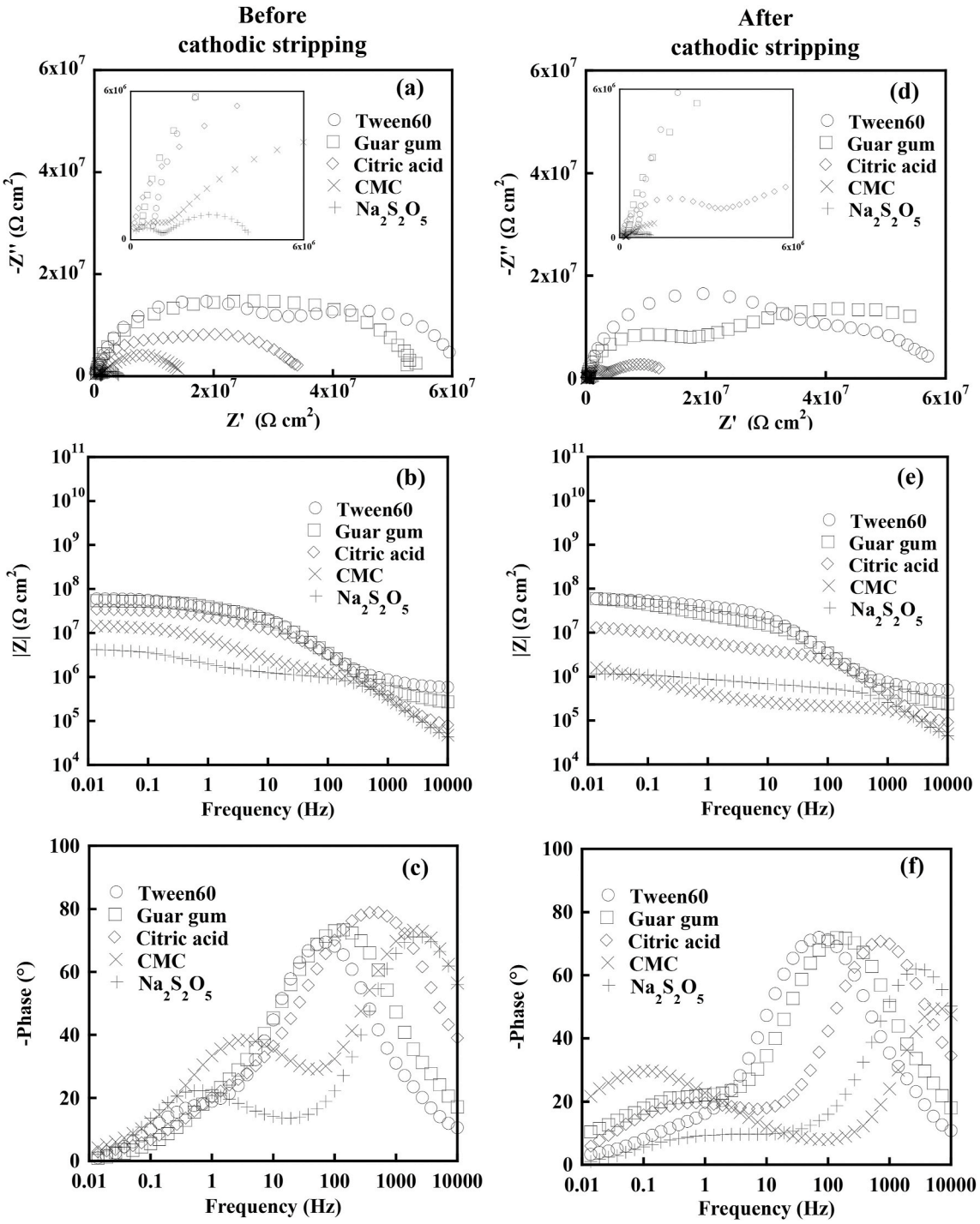

Fig. 6. Impedance diagrams of five food additives in epoxy-phenolic coated tinplate cans for sterilized conditions. (a) Nyquist, (b) Bode modulus, (c) Bode phase plots before cathodic stripping, (d) Nyquist, (e) Bode modulus, and (f) Bode phase plots after cathodic stripping at −6 V (Ag/AgCl).

containing CMC and $Na_2S_2O_5$, after cathodic stripping. Macroscopic images of the blisters found in the cases of CMC and $Na_2S_2O_5$ are illustrated in Fig. 7a and b, respectively. Vigorous blisters were observed after sterilization, comparing between Fig. 4 (non-sterilized) and Fig. 7 (sterilized).

SEM cross-sectional images and EDS analysis of blisters of $Na_2S_2O_5$ and CMC after sterilization and after cathodic stripping are illustrated in Fig. 8a and b, respectively. In the case of $Na_2S_2O_5$, corrosion product was clearly seen in the middle of the blister, whereas in the case of CMC, it was found only at the interface between the coating and substrate. EDS analysis showed that corrosion product was in a form of iron oxide.

3.3. Equivalent electrical circuit model evaluation

Equivalent electrical circuit (EEC) models were used to quantitatively analyze a degree of coating degradation. According to the results shown in Sections 3.1 and 3.2, fitted EEC could be categorized into two models as illustrated in Fig. 9; Fig. 9a shows the fitted EEC of control electrolyte (distilled water) and Fig. 9b displays that of food additives. Each fitted EEC model represented both for non-sterilized and sterilized conditions as well as for before and after cathodic stripping. Fitted values ($p < 0.05$) of all cases are shown in Table 4.

According to the fitted EEC model for control electrolyte, as

Table 3
Blister formation in epoxy-phenolic coated tinplate cans with sterilized conditions.

Food additives	Blisters (sterilized condition)	
	Before cathodic stripping	After cathodic stripping
Distilled water (control)	No	No
Tween 60	No	No
Guar gum	No	No
Citric acid	No	No
CMC	No	Yes (large)
$Na_2S_2O_5$	No	Yes (small)

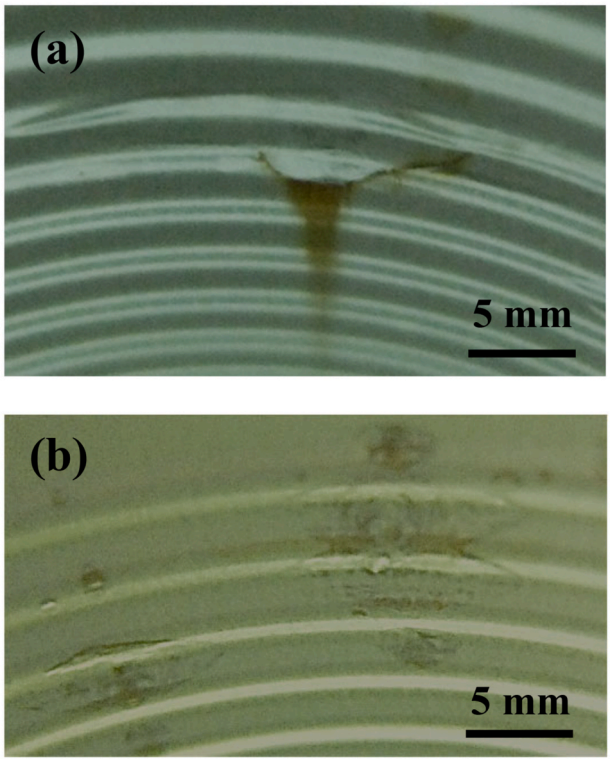

Fig. 7. Macroscopic images of blisters in sterilized cans containing (a) CMC and (b) $Na_2S_2O_5$ after cathodic stripping at −6 V (Ag/AgCl).

displayed in Fig. 9a, it represented a high performance coating. R_e is the electrolyte resistance, R_c is the coating resistance, Q_c is the coating capacitance. A constant phase element (Q_c) was used in this work in order to consider the divergence from pure capacitance. R_c decreased after the sterilization process and after cathodic stripping. However, R_c was still higher than 10^6 Ω cm^2 and blisters could not be observed (see Sections 3.1.3 and 3.2.3). A previous study reported that blisters/corrosion of metal were observed when R_c was less than 10^6 Ω cm^2 (Forsgren, 2006; Husain et al., 2017). It suggested that distilled water should not be a cause of blister formation in the epoxy-phenolic coated tinplate can.

In the case of fitted EEC model for food additives, as seen in Fig. 9b, electrolyte penetrated into the coating and formed a new liquid/metal interface under the coating. Another RQ was added to represent the electrochemical behavior of the coating/metal interface at low frequency of the impedance diagram (Deflorian et al., 1996; Madhankumar et al., 2012). R_{ct} is the charge transfer resistance of the corrosion process at the coating/substrate interface and Q_{dl} is the capacitance of the electrochemical double layer appearing when the electrolyte penetrates into the coating and forms a new liquid/metal interface under the coating (CatalÁ et al., 1998).

According to the fitted values as illustrated in Table 4, in the case of non-sterilized condition, R_c of tween 60 was higher than that of guar gum, citric acid, CMC, and $Na_2S_2O_5$, respectively. This trend was similar both before and after cathodic stripping. CMC and $Na_2S_2O_5$ were the food additives that showed the lowest R_c value, especially after cathodic stripping. The higher R_c indicated the higher ionic barrier of the coating and the higher resistance to penetration of electrolyte (O'Donoghue et al., 2003). R_c decreased when the electrolyte entered into the pores of the coating, especially after applying a potential because of the expansion of pores (Loveday et al., 2004a; Waters et al., 2014). Thus, CMC and $Na_2S_2O_5$ were the most powerful food additives that disrupted the ionic barrier of the epoxy-phenolic coating and diminished the coating performance.

Q_c of each food additive were similar for both before and after cathodic stripping, but after cathodic stripping they were slightly higher. Higher values of Q_c indicated a higher water content in the coating (O'Donoghue et al., 2003). Hence, the epoxy-phenolic coating absorbed more food additives after cathodic stripping.

R_{ct} was created due to the occurrence of a charge transfer reaction at the coating/metal interface when the electrolyte solution contacted with the metal substrate. The charge transfer reaction caused corrosion on the substrate and the lower R_{ct} value indicated a higher corrosion rate of the metal (Loveday et al., 2004b; O'Donoghue et al., 2003). From Table 4, it can be seen that the R_{ct} of all food additives decreased after cathodic stripping, except for tween 60. This indicated that, after cathodic stripping, tween 60 solution did not further activate the charge transfer reaction at the coating/metal interface. Other food additives could provoke the charge transfer reaction at the coating/metal interface, especially $Na_2S_2O_5$, which had the lowest R_{ct} value.

When electrolyte penetrated into the coating and it was over the metal substrate, the Q_{dl} parameter appeared. A higher Q_{dl} value indicated a greater wetted area of substrate (O'Donoghue et al., 2003). From Table 4, it suggested that CMC and $Na_2S_2O_5$ could easily reach the metal substrate compared to the others, especially after cathodic stripping.

After sterilization, R_c decreased corresponding with an increase in Q_c, as well as a decrease in R_{ct} in association with an increase in Q_{dl}, especially after cathodic stripping. This indicated that the heat and pressure during the sterilization process deteriorated the coating leading to a higher permeation of food additives into the coating. CMC and $Na_2S_2O_5$ showed that they were the most aggressive food additives and they were capable of penetrating into the coating.

4. Discussion

Considering the pH of each food additive solution as shown in Table 1, it seemed that pH had less influence on blister formation; pH of citric acid solution was the lowest (pH = 3.2), but blister could not be detected in every condition studied. The results revealed that CMC and $Na_2S_2O_5$ were the major causes of blister formation in the processed coconut milk cans as compared to other food additives. Regarding the chemical structures of CMC and $Na_2S_2O_5$, it shows that dissolution of both food additives in water produced Na^+ ions in the solution, whereas other additives did not. CMC was used in the form of a sodium salt and the dissolved $Na_2S_2O_5$ in water generated Na^+ ions and SO_2, as shown in Equations (1) and (2). Thus, Na^+ ions were likely to be one of the key factors to accelerate blister formation in the epoxy-phenolic coated tinplate can used for the processed coconut milk product.

$$Na_2S_2O_5 + H_2O \Leftrightarrow 2Na^+ + 2HSO_3^- \quad (1)$$

$$HSO_3^- + H^+ \Leftrightarrow SO_2 + H_2O \quad (2)$$

Water could penetrate into microscopic pores, cracks, and defects in the coating, especially coatings containing polar molecules. Water could also enter into the high density or cross-linked paint through a low molecular weight channel between the high-density segment and low cross-linked area (Nguyen et al., 1996; Tator, 2015). Water uptake in the coating caused a conductive pathway formation allowing ions to be

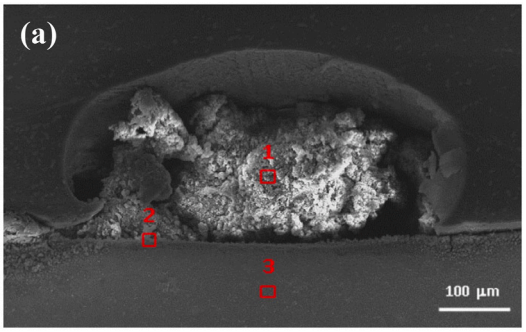

Position	Wt. (%)			
	C	O	Sn	Fe
1	32	24	-	16
2	13	11	5.4	66
3	3.8	-	-	96

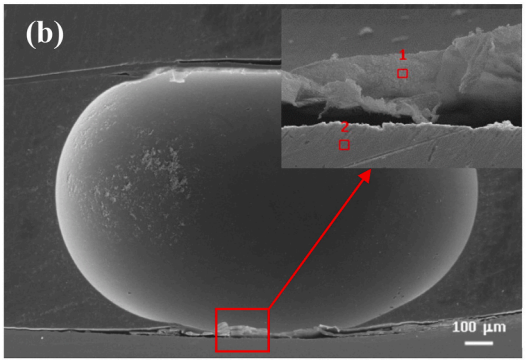

Position	Wt. (%)			
	C	O	Sn	Fe
1	57	30	5.0	8.0
2	5	-	-	95

Fig. 8. SEM cross-sectional images of blisters and EDS point analysis of (a) sterilized can with $Na_2S_2O_5$, and (b) sterilized can with CMC after cathodic stripping at −6 V (Ag/AgCl).

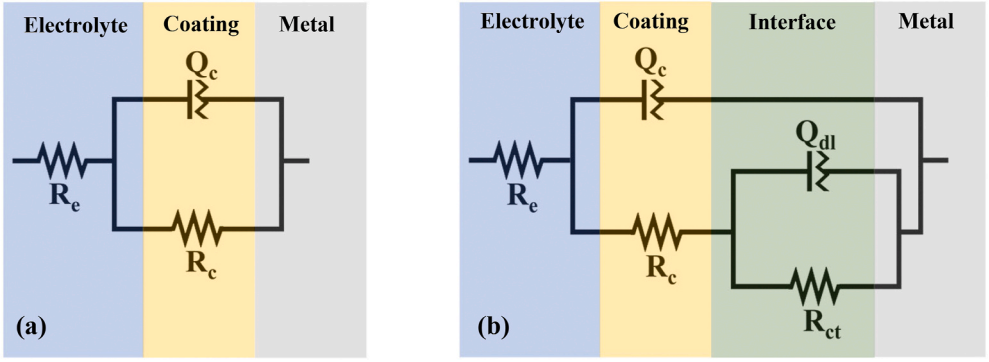

Fig. 9. Equivalent electrical circuit models of the epoxy-phenolic tinplate cans containing (a) distilled water and (b) food additives (tween 60, guar gum, citric acid, CMC, and $Na_2S_2O_5$) for non-sterilized and sterilized conditions as well as before and after cathodic stripping at −6 V (Ag/AgCl).

Table 4
Fitted values of non-sterilized and sterilized conditions of epoxy-phenolic coated tinplate cans containing distilled water and different food additives.

Food additives	Before cathodic stripping				After cathodic stripping			
	R_c (MΩ cm^2)	Q_c (µF/cm^2)	R_{ct} (MΩ cm^2)	Q_{dl} (mF/cm^2)	R_c (MΩ cm^2)	Q_c (µF/cm^2)	R_{ct} (MΩ cm^2)	Q_{dl} (mF/cm^2)
Non-sterilized condition								
Distilled water (control)	1252 ± 391	48 ± 6	–	–	152 ± 45	53 ± 1	–	–
Tween 60	114 ± 30	51 ± 0	79 ± 1	1 ± 0	117 ± 24	57 ± 0	77 ± 8	2 ± 0
Guar gum	30 ± 7	51 ± 4	108 ± 34	2 ± 0	20 ± 9	54 ± 5	14 ± 1	12 ± 0
Citric acid	16 ± 6	58 ± 6	27 ± 5	2 ± 0	7 ± 0	66 ± 10	14 ± 1	9 ± 1
CMC	5 ± 1	48 ± 4	48 ± 1	1 ± 0	2 ± 1	65 ± 1	7 ± 4	53 ± 35
$Na_2S_2O_5$	3 ± 0	54 ± 1	5 ± 1	16 ± 1	2 ± 0	63 ± 9	3 ± 0	21 ± 0
Sterilized conditions								
Distilled water (control)	103 ± 23	52 ± 1	–	–	51 ± 0	51 ± 0	–	–
Tween 60	30 ± 4	67 ± 3	28 ± 3	2 ± 0	30 ± 8	65 ± 0	20 ± 3	4 ± 1
Guar gum	21 ± 10	71 ± 2	20 ± 2	0.9 ± 0.1	15 ± 5	70 ± 2	40 ± 1	2 ± 0
Citric acid	10 ± 5	73 ± 5	17 ± 3	2 ± 1	6 ± 3	71 ± 1	10 ± 4	5 ± 2
CMC	5 ± 2	50 ± 0	25 ± 2	2 ± 0	0.2 ± 0	85 ± 1	2 ± 0	103 ± 12
$Na_2S_2O_5$	1 ± 0	87 ± 1	2 ± 1	27 ± 11	0.3 ± 0.2	128 ± 21	0.4 ± 0.1	130 ± 68

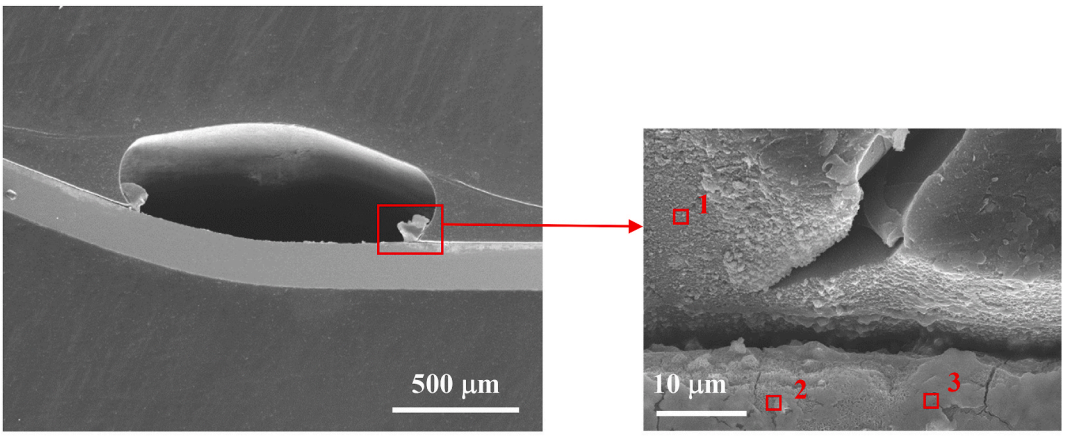

Position	Wt. (%)					
	C	O	Sn	Fe	Na	S
1	59	18	-	22	0.5	-
2	10	25	2.4	60	2.2	-
3	14	32	9.1	40	3.6	0.9

Fig. 10. SEM cross-sectional images of blister and EDS point analysis of sterilized can containing a mixture of $Na_2S_2O_5$ and CMC after cathodic stripping at −6 V (Ag/AgCl).

transported through the coating to the substrate surface. After the conductive pathway was created in the coating, Na^+ ions could reach the metal surface by this route. Especially, after promotion by the applied potential, the diffusion of Na^+ ions, water and oxygen was facilitated (Deflorian and Rossi, 2006; Nguyen et al., 1995). The increase of Na^+ ingress through the coating led to the lowering of the ionic resistance of the coating, or a reduction of the barrier properties of the coating. However, the Na^+ ions were not found at the tinplate substrate which might be due to the low concentration of Na^+ ions that passed though the coating. In order to confirm that Na^+ ions passed though the coating, a further investigation was carried out with a mixture of $Na_2S_2O_5$ and CMC solution at concentration of each additive, as illustrated in Table 1, in order to increase an aggressiveness of the electrolyte and still remain the real concentration used in the industry. As expected, blisters were found and EDS analysis of cross-sectional blister, as illustrated in Fig. 10, revealed a presence of Na element at the tinplate metal. During the progress of conductive pathways and the access of Na^+ ions to the metal substrate, the corrosion process at the metal surface was simultaneously initiated. The presence of a galvanic corrosion cell (Sn–Fe) in the epoxy-phenolic tinplate can is a standard situation.

There have been two main proposed corrosion mechanisms of the tinplate. In a deaerated system, the corrosion of tinplate was dominated by the anodic dissolution of tin coating (Sn acted as anode and Fe acted and cathode), whereas in an aerated system, the dissolution of steel substrate was dominated (Fe acted as anode and Sn acted as cathode) (e.g. Zhou et al., 2017). However, the inversion of polarity of Sn–Fe was also found depending on the chelating anion in the food product, influencing the corrosion mechanism (Freire et al., 2016). Furthermore, with naturally-aerated condition, a codissolution of Fe and Sn occurred at the beginning stage of the corrosion process followed by the dissolution of Fe (Wang et al., 2019).

In this work, the internal tin coating mass was 1.10 gm^{-2} which was quite low and the tin layer was not clearly observed. A low coating mass caused an ununiformed tin layer (Wu et al., 2018). Less thickness of tin coating occurred on rougher surface and on beads of the can, leading to more areas of steel exposed to the electrolyte. With the naturally-aerated system and a thin layer of tin coating in this work, steel was soon exposed to the conductive pathways, dissolution of steel occurred as shown in Equation (3). Oxygen reduction took place at the cathodic region producing hydroxide ions (OH^-) as shown in Equation (4). In addition, the reduction of oxygen was also encouraged by the applied potential used in this work leading to an increased transportation of cations (Na^+) to the cathodic area in order to balance the charge at the interface, as illustrated in Equation (5).

$$Fe \rightarrow Fe^{2+} + 2e^- \quad (3)$$

$$\frac{1}{2}O_2 + H_2O + 2e^- \rightarrow 2OH^- \quad (4)$$

$$\frac{1}{2}O_2 + H_2O + 2Na^+ + 2e^- \rightarrow 2(Na^+OH^-) \quad (5)$$

The formation of strong alkalinity (NaOH) at the cathodic site caused the initiation of coating delamination, called cathodic delamination. Then, the alkaline solution accumulated at the interface resulting in blister formation and the blistering was accelerated by osmotic pressure resulting from the concentration gradient. Therefore, the blisters were only found in the tinplate cans tested with the solutions containing Na^+ions, which were CMC and $Na_2S_2O_5$. Furthermore, pitting corrosion occurred beneath of the coating and corrosion product was then produced inside the blister and the coating was finally failed and broken, visibly by naked eyes, as illustrated in Fig. 7. Pitting corrosion was also found by Dey and Agrawal (2018) in epoxy-phenolic lacquered tinplate when the tin coating mass was lower than 5.6 gm^{-2}.

Generally, it is well known that blisters/corrosion do not appear in the food can coated with epoxy-phenolic lacquer containing NaCl solution. However, in this work, blisters/corrosion were found in the case of $Na_2S_2O_5$ and CMC. Another factor that accelerated the corrosion of tinplate can, in the case of $Na_2S_2O_5$, was generated SO_2 as displayed in Equation (2). SO_2 acted as a corrosion accelerator in an acid medium which led to more dissolution of tin, promoting highly exposed steel

substrate and followed by dissolution of steel. In addition, $Na_2S_2O_5$ is a reducing agent. The SO_2 could react with water and produce the HSO_3^- anion which initiated the oxidation reaction at the interface, as shown in Equations (6) and (7). Then, the electrons moved to cathodic sites resulting in a flow of galvanic current. These resulted in an aggressive corrosion attack.

$$SO_2 + H_2O \rightarrow H_2SO_3 \rightarrow HSO_3^- + H^+ \quad (6)$$

$$HSO_3^- + H_2O \rightarrow HSO_4^- + 2H^+ + 2e^- \quad (7)$$

Furthermore, the larger blisters seen in CMC might be due to the fact that CMC contains the carboxylate group (COO^-) in the structure. The carboxylate groups interacted with hydrogen of the hydroxyl groups of the coating via hydrogen bonds. Oxygen atoms in the coating also formed hydrogen bonds with hydrogen of the hydroxyl groups in the cellulose structure. So, the epoxy-phenolic coating was damaged after CMC diffused into the defects. Additionally, after CMC reached the metal substrate, the interaction between the metal ions and the carboxylate groups, as a coordinate bond, increased (Escaig, 1993). This interaction was attracted to the metal better than the interaction of the metal substrate with the oxygen atoms in the coating (Zhang, 1995). Consequently, the loss of adhesion between the epoxy-phenolic coating and the metal was observed, with a higher accumulation of electrolyte at the coating/metal interface.

5. Conclusions

Food additives that gave Na^+ ions to the solutions, $Na_2S_2O_5$ and CMC, were the most aggressive food additives. Blisters were only found in the epoxy-phenolic coated tinplate cans containing $Na_2S_2O_5$ and CMC after the applied potential, for both non-sterilized and sterilized conditions. Na^+ ions played an important role in initiating and accelerating the blister formation. Although the heat and pressure generated during the sterilization process reduced the efficiency of the epoxy-phenolic coating on the can, without food additives, blisters did not form even after the applied potential.

Credit Author statement

Duangkamol Promlok: Investigation, writing-original draft. **Noparat Kanjanaprayut**: Conceptualization, methodology, resources. **Nuntawat Kiatisereekul**: Conceptualization. **Ratana Chanthateyanonth**: Writing-review & editing. **Manthana Jariyaboon**: Supervision, writing-review & editing.

Declaration of competing interest

The authors declare that they have no known competing financial interests or personal relationships that could have appeared to influence the work reported in this paper.

Acknowledgements

The authors would like to thank Lohakij Rung Charoen Sub Co., Ltd., Thailand for providing the epoxy-phenolic coated tinplate cans, information of food additives, and for the help of sterilizing process. Duangkamol Promlok acknowledges the Science Achievement Scholarship of Thailand (SAST) for her financial support. This research is funded by the Science Achievement Scholarship of Thailand (SAST).

Appendix A. Supplementary data

Supplementary data to this article can be found online at https://doi.org/10.1016/j.jfoodeng.2021.110513.

References

Amirudin, A., Thieny, D., 1995. Application of electrochemical impedance spectroscopy to study the degradation of polymer-coated metals. Prog. Org. Coating 26 (1), 1–28. https://doi.org/10.1016/0300-9440(95)00581-1.

CatalÁ, R., CabaÑEs, J.M., Bastidas, J.M., 1998. An impedance study on the corrosion properties of lacquered tinplate cans in contact with tuna and mussels in pickled sauce. Corrosion Sci. 40 (9), 1455–1467. https://doi.org/10.1016/S0010-938X(98)00050-X.

Charbonneau, J.E., 1997. Recent case histories of food product-metal container interactions using scanning electron microscopy-X-ray microanalysis. Scanning 19 (7), 512–518. https://doi.org/10.1002/sca.4950190710.

Charbonneau, J.E., 2001. Investigation of corrosion and container integrity in metal food containers using scanning electron microscopy-X-ray microanalysis. Scanning 23 (3), 198–203. https://doi.org/10.1002/sca.4950230306.

Deflorian, F., Fedrizzi, L., Bonora, P.L., 1996. Influence of the photo-oxidative degradation on the water barrier and corrosion protection properties of polyester paints. Corrosion Sci. 38 (10), 1697–1708. https://doi.org/10.1016/S0010-938X(96)00062-5.

Deflorian, F., Rossi, S., 2006. An EIS study of ion diffusion through organic coatings. Electrochim. Acta 51 (8), 1736–1744. https://doi.org/10.1016/j.electacta.2005.02.145.

Dey, S., Agrawal, M.K., 2018. Evaluation of lacquered tinplate corrosion in canned food through characterization by using SEM & EDS technique. Int. J. Eng. Technol. 7 (4.5), 341–346. https://doi.org/10.14419/ijet.v7i4.5.20103.

Doherty, M., Sykes, J.M., 2004. Micro-cells beneath organic lacquers: a study using scanning Kelvin probe and scanning acoustic microscopy. Corrosion Sci. 46 (5), 1265–1289. https://doi.org/10.1016/j.corsci.2003.09.016.

Escaig, B., 1993. Binding metals to polymers. A short review of basic physical mechanisms. J. Phys. IV 3, 753–761. https://doi.org/10.1051/jp4:19937120.

Feng, Z., Frankel, G.S., 2016. Evaluation of coated Al alloy using the breakpoint frequency method. Electrochim. Acta 187, 605–615. https://doi.org/10.1016/j.electacta.2015.11.114.

Forsgren, A., 2006. Corrosion Testing - Practice, *Corrosion Control through Organic Coatings*. CRC Press, Florida, pp. 365–463.

Freire, M.T.A., Petrus, R.R., Gatti, J.A.B., Leite, M.F.B., Kunitake, M.T., Freire, C.M.A., 2016. Food-packaging interaction on the stability of canned sweetened cupuacu (*Theobroma grandiflorum schum.*) Puree. Revista Coatinga 29 (4), 1006–1014. https://doi.org/10.1590/1983-21252016v29n426rc.

Grassino, A.N., Grabarić, Z., Pezzani, A., Squitieri, G., Berkovic, K., 2010. Corrosion inhibition with different protective layers in tinplate cans for food preservation. J. Sci. Food Agric. 90, 2419–2426. https://doi.org/10.1002/jsfa.4101.

Grundmeier, G., Schmidt, W., Stratmann, M., 2000. Corrosion protection by organic coatings: electrochemical mechanism and novel methods of investigation. Electrochim. Acta 45 (15), 2515–2533. https://doi.org/10.1016/S0013-4686(00)00348-0.

Husain, A., Chakkamalayath, J., Al-Bahar, S., 2017. Electrochemical impedance spectroscopy as a rapid technique for evaluating the failure of fusion bonded epoxy powder coating. Eng. Fail. Anal. 82, 765–775. https://doi.org/10.1016/j.engfailanal.2017.06.041.

Jafari, S.M., Amanjani, M., Ganjeh, M., Katouzian, I., Sharifi, N., 2018. The influence of storage time and temperature on the corrosion and pressure changes within tomato paste cans with different filling rates. J. Food Eng. 228, 32–37. https://doi.org/10.1016/j.jfoodeng.2018.02.008.

Jianguo, L., Gaoping, G., Chuanwei, Y., 2005. EIS study of corrosion behavior of organic coating/Dacromet composite systems. Electrochim. Acta 50 (16), 3320–3332. https://doi.org/10.1016/j.electacta.2004.12.010.

Kogure, M., Inada, Y., Takahashi, H., Shimoda, M., 2019. Proposed mechanism for uneven detinning in cans of Satsuma Mandarin (citrus unshiu). J. Food Eng. 261, 9–14. https://doi.org/10.1016/j.jfoodeng.2019.05.005.

Kontominas, M.G., Prodromidis, M.I., Paleologos, E.K., Badeka, A.V., Georgantelis, D., 2006. Investigation of fish product–metal container interaction using scanning electron microscopy–X-ray microanalysis. Food Chem. 98 (2), 225–230. https://doi.org/10.1016/j.foodchem.2005.06.004.

Li, Y., Yang, Z., Qiu, H., Dai, Y., Zheng, Q., Li, J., Yang, J., 2014. Self-aligned graphene as anticorrosive barrier in waterborne polyurethane composite coatings. J. Mater. Chem. 2 (34), 14139–14145. https://doi.org/10.1039/C4TA02262A.

Loveday, D., Peterson, P., Rodgers, B., 2004a. Evaluation of organic coatings with electrochemical impedance spectroscopy - Part 1: fundamentals of electrochemical impedance spectroscopy. J. Coating Technol. 1 (8), 46–52.

Loveday, D., Peterson, P., Rodgers, B., 2004b. Evaluation of organic coatings with electrochemical impedance spectroscopy - Part 2: application of EIS to coatings. J. Coating Technol. 1 (10), 88–93.

Madhankumar, A., Nagarajan, S., Rajendran, N., Nishimura, T., 2012. EIS evaluation of protective performance and surface characterization of epoxy coating with aluminum nanoparticles after wet and dry corrosion test. J. Solid State Electrochem. 16 (6), 2085–2093. https://doi.org/10.1007/s10008-011-1623-1.

Maharatanaviroj, R., Supapan, T., Pungwiwat, N., Kanjanaprayut, N., 2016. Evaluation of corrosion failure of lacquer coated food can by electrochemical and microscopic food. J. Appl. Sci. 15 (1), 46–61. https://doi.org/10.14416/j.appsci.2016.04.001.

Marikkar, J.M.N., Madurapperuma, W.S., 2012. Coconut. In: Siddiq, M. (Ed.), Tropical and Subtropical Fruits. Wiley-Blackwell, pp. 159–177. https://doi.org/10.1002/9781118324097.ch9.

Nguyen, T., Hubbard, J.B., Pommersheim, J.M., 1996. Unified model for the degradation of organic coatings on steel in a neutral electrolyte. In: Proceedings of Annual

Meeting of the Federation of Societies for Coatings Technology, vol. 68. JCT: Journal of Coating Technology, pp. 45–56, 855.
Nguyen, T., Zhang, Z., Lin, C., Pommersheim, J.M., 1995. Cation diffusion at the polymer coating/metal interface. J. Adhes. Sci. Technol. 9 (7), 935–951. https://doi.org/10.1163/156856195X00806.
O'Donoghue, M., Garrett, R., Datta, V., Roberts, P., Aben, T., 2003. Electrochemical impedance spectroscopy: testing coatings for rapid immersion service. Mater. Perform. 42, 36–41.
Page, B., Edwards, M., May, N., 2003. Metal cans. In: Coles, R., McDowell, D., Kirwan, M. J. (Eds.), Food Packaging Technology. Wiley-Blackwell, Oxford, pp. 121–151.
Popov, B.N., Alwohaibi, M., White, R.E., 1993. Using electrochemical impedance spectroscopy as a tool for organic coating solute saturation monitoring. J. Electrochem. Soc. 140 (4), 947–951. https://doi.org/10.1149/1.2056233.
Pournaras, A.V., Prodromidis, M.I., Katsoulidis, A.P., Badeka, A.V., Georgantelis, D., Kontominas, M.G., 2008. Evaluation of lacquered tinplated cans containing octopus in brine by employing X-ray microanalysis and electrochemical impedance spectroscopy. J. Food Eng. 86 (3), 460–464. https://doi.org/10.1016/j.jfoodeng.2007.09.034.
Rikhari, B., Mani, S.P., Rajendran, N., 2016. Investigation of corrosion behavior of polypyrrole-coated Ti using dynamic electrochemical impedance spectroscopy (DEIS). RSC Adv. 6 (83), 80275–80285. https://doi.org/10.1039/C6RA09100H.
Tator, K.B., 2015. Coating deterioration. In: Tator, K.B. (Ed.), Protective Organic Coatings. ASM International, Ohio, pp. 462–473. https://doi.org/10.31399/asm.hb.v05b.a0006073.
Upadhyay, V., Wiering, L., Bergseth, Z., Qi, X., Battocchi, D., 2020. Corrosion beneath a blister with high impedance. J. Coat. Technol. Res. 17, 1105–1111. https://doi.org/10.1007/s11998-019-00280-9.
VerÍssimo, M.I.S., Silva, R.P.O., Gomes, M.T.S.R., 2016. Iron migration from undamaged and dented juice tinplate cans. J. Sci. Food Agric. 96, 3042–3046. https://doi.org/10.1002/jsfa/7474.
Wang, J., Zhang, L., Gao, Y., Hu, W., 2019. Influence of storage temperature on the corrosion behavior of tinplate in citric acid solution. International Journal of Electrochemical Science 14, 59–74. https://doi.org/10.20964/2019.01.24.
Wang, K., Wang, J., Wang, H., Fu, C., Xia, D., Zheng, X., Dang, L.H., Shi, J.B., 2014. Corrosion detection of tinplate cans containing coffee using EIS/EN sensor. J. Cent. S. Univ. 21 (1), 76–82. https://doi.org/10.1007/s11771-014-1918-3.
Waters, N., Connolly, R., Brown, D., Laskows, B.C., 2014. Electrochemical impedance spectroscopy for coating evaluation using a micro sensor. In: Proceedings of Annual Conference of the Prognostics and Health Management Society 2014 (Texas, USA).
Wu, F.J., Liu, X.J., Xiao, X., 2018. Surface characterization of electroplated tinplate with different coating mass. Surf. Eng. 34 (6), 462–467. https://doi.org/10.1080/02670844.2017.1288343.
Xia, D., Song, S., Gong, W., Jiang, Y., Gao, Z., Wang, J., 2012. Detection of corrosion-induced metal release from tinplate cans using a novel electrochemical sensor and inductively coupled plasma mass spectrometer. J. Food Eng. 113 (1), 11–18. https://doi.org/10.1016/j.jfoodeng.2012.05.035.
Zhang, Y., 1995. Adhesion of Epoxy Coatings to an Alloy-Coated Steel Sheet, *Doctor of Philosophy thesis*. Department of Materials Engineering, University of Wollongong. http://ro.uow.edu.au/theses/1481.
Zhang, Y., Tian, J., Zhong, J., Shi, X., 2018. Thin nacre-biomimetic coating with super-anticorrosion performance. ACS Nano 12 (10), 10189–10200. https://doi.org/10.1021/acsnano.8b05183.
Zhou, C., Wang, J., Song, S., Xia, D., Wang, K., Shen, C., Luo, B., Shi, J., 2013. Degradation mechanism of lacquered tinplate in energy drink by in-situ EIS and EN. J. Wuhan Univ. Technol.-Materials Sci. Ed. 28 (2), 367–372. https://doi.org/10.1007/s11595-013-0697-2.
Zhou, D., Wang, J., Han, Z., Liu, X., Mao, J., 2017. Corrosion behavior of tinplate in aerated and deaerated NaCl solution. International Journal of Electrochemical Science 12, 631–651. https://doi.org/10.20964/2017.01.23.